

# Degenerate limit thermodynamics beyond leading order for models of dense matter

Constantinos Constantinou<sup>1</sup>

*Institute for Advanced Simulation, Institut für Kernphysik, and Jülich Center  
for Hadron Physics, Forschungszentrum Jülich, D-52425 Jülich, Germany*

Brian Muccioli<sup>2</sup>

*Department of Physics and Astronomy, Ohio University, Athens, OH 45701*

Madappa Prakash<sup>3</sup>

*Department of Physics and Astronomy, Ohio University, Athens, OH 45701*

James M. Lattimer<sup>4</sup>

*Department of Physics and Astronomy, Stony Brook University, Stony Brook, NY  
11794-3800*

---

## Abstract

Analytical formulas for next-to-leading order temperature corrections to the thermal state variables of interacting nucleons in bulk matter are derived in the degenerate limit. The formalism developed is applicable to a wide class of non-relativistic and relativistic models of hot and dense matter currently used in nuclear physics and astrophysics (supernovae, proto-neutron stars and neutron star mergers) as well as in condensed matter physics. We consider the general case of arbitrary dimensionality of momentum space and an arbitrary degree of relativity (for relativistic mean-field theoretical models). For non-relativistic zero-range interactions, knowledge of the Landau effective mass suffices to compute next-to-leading order effects, but in the case of finite-range interactions, momentum derivatives of the Landau effective mass function up to second order are required. Numerical computations are performed to compare results from our analytical formulas with the exact results for zero- and finite-range potential and relativistic mean-field theoretical models. In all cases, inclusion of next-to-leading order temperature effects substantially extends the ranges of partial degeneracy for which the analytical treatment remains valid.

---

<sup>1</sup>c.constantinou@fz-juelich.de

<sup>2</sup>bm956810@ohio.edu

<sup>3</sup>prakash@ohio.edu

<sup>4</sup>james.lattimer@stonybrook.edu

*Keywords:* Hot and dense matter, thermal effects, potential and field-theoretical models.

---

## 1. INTRODUCTION

Homogeneous bulk matter comprised of fermions is commonly encountered in astrophysics, condensed matter physics, and nuclear physics. For extreme degenerate to near-degenerate conditions which prevail when the temperature is small compared to the Fermi temperature, Landau's Fermi Liquid Theory (FLT) has been a useful guide to describe the thermodynamic and transport properties of the system (see, *e.g.*, [1] and references therein). The equation of state (EOS) of dense matter in cold and catalyzed neutron stars, for example, is dominated by the zero-temperature properties (which predominantly determine the structure of and neutrino interactions within the star) while finite-temperature corrections (important for the cooling of neutron stars) are adequately given by the degenerate limit expressions from FLT. The leading order FLT corrections to the energy density and pressure are quadratic in the temperature; corrections to the entropy and specific heats are linear in the temperature. However, matter in supernovae and proto-neutron stars [2, 3], especially in situations in which collapse to a black hole occurs, may reach temperatures exceeding the Fermi temperature, in which case the finite-temperature contributions extend beyond those given by the FLT. In neutron star mergers, it is likely that in some cases a hyper-massive neutron star, or HMNS, is formed: the merged remnant mass exceeds the cold maximum mass. The metastable support is provided by rotation, including differential rotation, and thermal effects. The timescale over which collapse to a black hole eventually occurs, potentially observable in gravitational wave signatures, will therefore be sensitive to thermal effects [4]. In this contribution, we derive analytical formulas for next-to-leading order temperature effects in the state variables of interacting nucleons in both the non-relativistic and relativistic limits for a variety of nuclear interaction models.

For non-relativistic models with zero-range interactions, knowledge of the Landau effective mass is sufficient to satisfy thermodynamic identities. However, in the general case of finite-range interactions, momentum derivatives of the Landau effective mass function up to second order are required. We compare results from the analytical expressions to exact numerical calculations for zero- and finite-range potential models as well as for relativistic mean-field theoretical models. The analytic next-to-leading order expressions lead to an improvement of the leading order results of FLT, as demonstrated by the wider ranges of degeneracy and temperature for which they remain valid. In addition, we derive relations in a form that are independent of the dimensionality of the momentum space under consideration. Therefore, although our discussion focuses on examples from dense matter physics, which are three-dimensional systems in momentum space, the expressions derived can have a wider application to certain problems in condensed matter physics in which the momentum space is two-dimensional.

The paper is organized as follows. In Sec. 2, the formalism to calculate next-to-leading order corrections to the results of FLT in D-dimensions is developed. Analytical formulas appropriate for 3-dimensions are given in Sec. 3, whereas  
45 Sec. 4 contains results for 2-dimensions. The formalism is applied to zero- and finite-range potential models and a relativistic field-theoretical model in Sec. 5. Numerical results for these models are presented in Sec. 6 where the extent to which the next-to-leading order corrections improve the FLT results are demonstrated. Section 7 presents a summary and conclusions. Useful formulas for the  
50 evaluation of the thermal properties are provided in Appendices A, B, and C.

## 2. GENERAL CONSIDERATIONS

For a generic Hamiltonian density  $\mathcal{H}(n, \tau)$  where  $n$  and  $\tau$  are the number and kinetic energy densities respectively, the single-particle potential  $U$  is obtained from a functional differentiation of  $\mathcal{H}$  with respect to  $n$ , and can contain terms  
55 depending on  $n$  as well as the momentum  $p$ :

$$U(n, p) = \frac{\delta \mathcal{H}}{\delta n} = \mathcal{U}(n) + R(p), \quad (1)$$

where  $\mathcal{U}(n)$  denotes contributions that depend on  $n$  only. Note that  $R$  above may also be  $n$ -dependent but we will suppress this for notational simplicity.

The study of the thermodynamic properties of a fermion system involves integrals of the form

$$I = \int_0^\infty dp g(p) f(p), \quad f(p) = \left[ 1 + \exp \left( \frac{\epsilon - \mu}{T} \right) \right]^{-1}, \quad (2)$$

60 where  $T$  is the temperature,  $\mu$  is the chemical potential, and the single-particle spectrum

$$\epsilon = \frac{p^2}{2m} + U(n, p). \quad (3)$$

The structure of the function  $g(p)$  is determined by the state variable under consideration. In general, integrals involving the Fermi function  $f(p)$  do not admit analytical solutions and thus require numerical treatment. In the low-  
65 temperature limit, however, when the degeneracy parameter

$$\eta = \frac{\mu - \epsilon(p=0)}{T} \quad (4)$$

is large, these integrals can be approximately evaluated employing the Sommerfeld expansion (see, *e.g.*, [5]) by transforming Eq. (2) to

$$I = \int_0^\infty dy \frac{\phi(y)}{1 + \exp(y - \eta)} \xrightarrow{\eta \gg 1} \int_0^\eta \phi(y) dy + \frac{\pi^2}{6} \left. \frac{d\phi}{dy} \right|_{y=\eta} + \frac{7\pi^4}{360} \left. \frac{d^3\phi}{dy^3} \right|_{y=\eta} + \dots \quad (5)$$

with the identification  $\phi(y)dy = g(p)dp$ , and the substitution

$$y \equiv \frac{\epsilon - \mathcal{U}(n)}{T} = \frac{p^2}{2mT} + \frac{R(p)}{T}, \quad (6)$$

from which it follows that

$$\frac{dy}{dp} = \frac{p}{\mathcal{M}T} \quad \text{and} \quad \phi(y) = \frac{\mathcal{M}T}{p} g(p), \quad (7)$$

70 where the Landau effective mass function

$$\mathcal{M}(p) = m \left[ 1 + \frac{m}{p} \frac{dR(p)}{dp} \right]^{-1}. \quad (8)$$

This function is implicitly temperature-dependent and its relation to the Landau effective mass  $m^*$  is

$$\mathcal{M}(p = p_F; T = 0) = m^*, \quad (9)$$

where  $p_F$  is the Fermi momentum. From the relations in Eq. (7)

$$\frac{d\phi}{dy} = -\frac{T^2 \mathcal{M}^2 g}{p^3} \left[ 1 - p \left( \frac{g'}{g} + \frac{\mathcal{M}'}{\mathcal{M}} \right) \right] \quad (10)$$

$$\begin{aligned} \frac{d^3\phi}{dy^3} &= -\frac{15T^4 \mathcal{M}^4 g}{p^7} \left[ 1 - p \left( \frac{g'}{g} + \frac{5}{3} \frac{\mathcal{M}'}{\mathcal{M}} \right) \right. \\ &+ \frac{2}{5} p^2 \left( \frac{g''}{g} + \frac{11}{3} \frac{\mathcal{M}' g'}{\mathcal{M} g} + \frac{11}{6} \frac{\mathcal{M}'^2}{\mathcal{M}^2} + \frac{7}{6} \frac{\mathcal{M}''}{\mathcal{M}} \right) \\ &- \frac{p^3}{15} \left( \frac{g'''}{g} + 7 \frac{\mathcal{M}'^2 g'}{\mathcal{M}^2 g} + 6 \frac{\mathcal{M}' g''}{\mathcal{M} g} + 4 \frac{\mathcal{M}'' g}{\mathcal{M} g} \right. \\ &\left. \left. + \frac{\mathcal{M}'^3}{\mathcal{M}^3} + \frac{\mathcal{M}'''}{\mathcal{M}} + 4 \frac{\mathcal{M}' \mathcal{M}''}{\mathcal{M}^2} \right) \right], \end{aligned} \quad (11)$$

75 where the primes denote differentiation with respect to  $p$ .

For a system in  $D$  dimensions having  $\gamma$  internal degrees of freedom, the number density is given by

$$n = C_D \int dp p^{D-1} f_p \quad \text{with} \quad C_D = \frac{\gamma}{(2\pi\hbar)^D} \frac{D\pi^{D/2}}{(D/2)!}. \quad (12)$$

The combination of Eqs. (5),(10), and (11) with  $g_n = p^{D-1}$  results in

$$\begin{aligned} n &= \frac{C_D}{D} \left\{ p_\mu^D + \frac{\pi^2}{6} D p_\mu^{D-4} \mathcal{M}_\mu^2 T^2 \left( D - 2 + p_\mu \frac{\mathcal{M}'_\mu}{\mathcal{M}_\mu} \right) \right. \\ &+ \frac{7\pi^4}{360} D p_\mu^{D-8} \mathcal{M}_\mu^4 T^4 \left[ (D-6)(D-4)(D-2) \right. \\ &\left. \left. + \left( \frac{p_\mu \mathcal{M}'_\mu}{\mathcal{M}_\mu} \right)^3 + (7D-18) \left( \frac{p_\mu \mathcal{M}'_\mu}{\mathcal{M}_\mu} \right)^2 \right] \right\} \end{aligned}$$

$$\begin{aligned}
& + (6D^2 - 40D + 59) \frac{p_\mu \mathcal{M}'_\mu}{\mathcal{M}_\mu} + \frac{p_\mu^3 \mathcal{M}'''_\mu}{\mathcal{M}_\mu} \\
& + 4 \frac{p_\mu^3 \mathcal{M}'_\mu \mathcal{M}''_\mu}{\mathcal{M}_\mu^2} + (4D - 11) \frac{p_\mu^2 \mathcal{M}''_\mu}{\mathcal{M}_\mu} \Big] + \dots \Big\} , \tag{13}
\end{aligned}$$

where the subscript  $\mu$  denotes quantities evaluated at  $\epsilon = \mu$ , *i.e.*,

$$\epsilon = \mu = \frac{p_\mu^2}{2m} + R(p_\mu) + \mathcal{U}(n). \tag{14}$$

80 For  $N$  particles in a volume  $V$ , the number density  $n = N/V$  at  $T = 0$  and at finite  $T$  is the same. Equating the result in Eq. (13) to its  $T = 0$  counterpart  $n = C_D p_F^3/D$ , and perturbatively inverting we get

$$p_\mu = p_F \left[ 1 - \frac{\pi^2}{6} \frac{m^{*2} T^2}{p_F^4} \left( D - 2 + \frac{p_F \mathcal{M}'_F}{m^*} \right) + \dots \right] \tag{15}$$

with

$$p_F = \left( \frac{nD}{C_D} \right)^{1/D} \quad \text{and} \quad \mathcal{M}'_F = \left. \frac{d\mathcal{M}}{dp} \right|_{p_F}. \tag{16}$$

As our main goal here is to derive the next-to-leading order correction in temperature for the entropy density  $s$ , it suffices to truncate the series expansion of  $p_\mu$  to  $\mathcal{O}(T^2)$ . We will show below that higher-order terms do not contribute at this level of approximation where we may also neglect the temperature dependence of  $\mathcal{M}$  and its derivatives. The result in Eq. (15) helps us to work only with quantities defined on the Fermi surface as done in Landau's Fermi-Liquid theory [1, 6, 7]. The entropy density is formally given by

$$s = -C_D \int dp p^{D-1} [f_p \ln f_p - (1 - f_p) \ln(1 - f_p)]. \tag{17}$$

Integrating this expression twice by parts we obtain

$$s = \frac{1}{T} \left\{ \frac{\tau}{m} \left( \frac{1}{2} + \frac{1}{D} \right) + n(\mathcal{U} - \mu) + C_D \int dp p^{D-1} f_p \left[ R(p) + \frac{p}{D} \frac{dR(p)}{dp} \right] \right\} \tag{18}$$

where

$$\tau = C_D \int dp p^{D+1} f_p \tag{19}$$

is the kinetic energy density. With the aid of Eq. (14) for the chemical potential, Eq. (18) can be written as

$$s = \frac{1}{T} \left\{ \frac{\tau}{m} \left( \frac{1}{2} + \frac{1}{D} \right) - n \frac{p_\mu^2}{2m} + C_D \int dp p^{D-1} f_p \left[ R(p) - R(p_\mu) + \frac{p}{D} \frac{dR(p)}{dp} \right] \right\} \tag{20}$$

95 from which we identify the functions

$$g_{1s}(p) = \frac{p^{D+1}}{m} \left( \frac{1}{2} + \frac{1}{D} \right) - p^{D-1} \frac{p_\mu^2}{2m} \quad (21)$$

$$g_{2s}(p) = p^{D-1} \left[ R(p) - R(p_\mu) + \frac{p}{D} \frac{dR(p)}{dp} \right] \quad (22)$$

to be used in the Sommerfeld expansion. For both of these functions, the first term on the right-hand side of Eq. (5) involving an integral vanishes yielding

$$\begin{aligned} s &= \frac{\pi^2}{3} C_D p_\mu^{D-2} \mathcal{M}_\mu T + \frac{7\pi^4}{90} C_D p_\mu^{D-6} \mathcal{M}_\mu^3 T^3 \left[ (D-4)(D-2) \right. \\ &\quad \left. + p_\mu^2 \frac{\mathcal{M}_\mu'^2}{\mathcal{M}_\mu^2} + p_\mu^2 \frac{\mathcal{M}_\mu''}{\mathcal{M}_\mu} + (3D-7)p_\mu \frac{\mathcal{M}_\mu'}{\mathcal{M}_\mu} \right]. \end{aligned} \quad (23)$$

Use of Eqs. (15) and (16) in the above result delivers the working expression for  $s$  in terms of quantities defined on the Fermi surface:

$$\begin{aligned} s &\simeq \frac{\pi^2}{3} C_D p_F^{D-2} m^* T + \frac{\pi^4}{45} C_D p_F^{D-6} m^{*3} T^3 \left[ (D-9)(D-2) \right. \\ &\quad \left. + \frac{7}{2} p_F^2 \frac{\mathcal{M}_F'^2}{m^{*2}} + \frac{7}{2} p_F^2 \frac{\mathcal{M}_F''}{m^*} + \frac{(16D-39)}{2} p_F \frac{\mathcal{M}_F'}{m^*} \right], \end{aligned} \quad (24)$$

100 where the  $\mathcal{O}(T)$  term is the well known result from FLT. We note that a large number of cancellations occur in obtaining Eqs. (23) and (24) despite the complexity of of Eqs. (10) and (11). For a system composed of different kinds of particles the total entropy density is a sum of the contributions from the individual species where, in Eq. (24), the Fermi momentum, the effective mass, and  
105 its derivatives all carry a particle-species index  $i$ .

Equation (24) forms the basis from which other properties of the system can be derived. For example, the entropy per particle is the simple ratio  $S = s/n$ , whereas the thermal energy, pressure, and chemical potential can be obtained through the application of the appropriate Maxwell relations [5]:

$$E_{th} = \int T dS, \quad P_{th} = -n^2 \int \frac{dS}{dn} dT \quad \text{and} \quad \mu_{th} = - \int \frac{ds}{dn} dT \quad (25)$$

110 [for a multiple-species system,  $\mu_{th,i} = - \int (ds/dn_i) dT$ ].

The specific heats at constant volume and pressure are given by the standard thermodynamics expressions [5]

$$C_V = T \left. \frac{\partial S}{\partial n} \right|_n = \left. \frac{\partial E_{th}}{\partial T} \right|_n \quad (26)$$

$$C_P = T \left. \frac{\partial S}{\partial n} \right|_P = C_V + \frac{T}{n^2} \left( \left. \frac{\partial P_{th}}{\partial T} \right|_n \right)^2 \frac{1}{\left. \frac{\partial P}{\partial n} \right|_T}. \quad (27)$$

We note that the formalism above has not considered effects, for example, from single particle-hole excitations, or from collective and pairing correlations near the Fermi surface [1, 8, 9]. Contributions from these sources must be added to those considered here when appropriate.

### 3. RESULTS FOR D=3

For a single-species system of spin 1/2 particles in 3 dimensions [for which  $C_3 = 1/(\pi^2 \hbar^3)$ ], the entropy density becomes

$$s = \frac{p_F m^* T}{3 \hbar^3} - \frac{2\pi^2}{15 \hbar^3} \frac{m^{*3} T^3}{p_F^3} (1 - L_F), \quad (28)$$

where

$$L_F \equiv \frac{7}{12} p_F^2 \frac{\mathcal{M}_F'^2}{m^{*2}} + \frac{7}{12} p_F^2 \frac{\mathcal{M}_F''}{m^*} + \frac{3}{4} p_F \frac{\mathcal{M}_F'}{m^*}. \quad (29)$$

We stress that, in general,

$$\left. \frac{d\mathcal{M}(p)}{dp} \right|_{p_F} = \mathcal{M}_F' \neq m^{*'} = \frac{d\mathcal{M}(p_F)}{dp_F} \quad (30)$$

as  $R$  can contain both  $p$  and  $p_F$  (via  $n$ ). In terms of the level-density parameter  $a = \pi^2 m^*/(2p_F^2) = \pi^2/(4T_F)$  (where  $T_F$  is the Fermi temperature), Eq. (28) can be written as

$$s = 2anT - \frac{16}{5\pi^2} a^3 n T^3 (1 - L_F). \quad (31)$$

The quantity  $L_F$  arises from nontrivial momentum dependencies in the single-particle potential. For free gases (where  $R(p) = 0$ ), and for systems having only contact interactions where  $R(p) \propto p^2$  (such as Skyrme models),  $L_F = 0$ .

Equation (31) in conjunction with Eqs. (25)-(27) leads to

$$S = 2aT - \frac{16}{5\pi^2} a^3 T^3 (1 - L_F), \quad E_{th} = aT^2 - \frac{12}{5\pi^2} a^3 T^4 (1 - L_F) \quad (32)$$

$$E_{th} = aT^2 - \frac{12}{5\pi^2} a^3 T^4 (1 - L_F) \quad (33)$$

$$P_{th} = \frac{2}{3} anQT^2 - \frac{8}{5\pi^2} a^3 nQT^4 \left( 1 - L_F + \frac{n}{2Q} \frac{dL_F}{dn} \right) \quad (34)$$

$$\mu_{th} = -a \left( 1 - \frac{2Q}{3} \right) T^2 + \frac{4}{5\pi^2} a^3 T^4 \left[ (1 - L_F)(1 - 2Q) - n \frac{dL_F}{dn} \right] \quad (35)$$

$$C_V = 2aT - \frac{48}{5\pi^2} a^3 T^3 (1 - L_F) \quad \text{and} \quad C_P = C_V + \frac{16}{9} \frac{a^2 Q^2 T^3}{\frac{dP_0}{dn}}, \quad (36)$$

where

$$Q = 1 - \frac{3n}{2m^*} \frac{dm^*}{dn}. \quad (37)$$

In the derivation of Eq. (36) we have assumed that the zero-temperature pressure  $P_0$  is such that  $dP_0/dn \gg dP_{th}/dn$ . This condition will not be met in

situations where  $P_0$  is relatively flat as in the vicinity of a critical point. When this is the case, we must use Eq. (27) for  $C_P$ , with

$$\left(\frac{\partial P_{th}}{\partial T}\Big|_n\right)^2 = \left(\frac{4}{3}anQT\right)^2 \left[1 - \frac{48}{5\pi^2}a^2T^2\left(1 - L_F + \frac{n}{2Q}\frac{dL_F}{dn}\right)\right] \quad (38)$$

$$\begin{aligned} \frac{\partial P}{\partial n}\Big|_T &= \frac{dP_0}{dn} + \frac{2}{3}aQT^2\left(1 - \frac{2Q}{3} + n\frac{dQ}{dn}\right) \\ &- \frac{5}{8\pi^2}a^3QT^4\left[\left(1 - 2Q + n\frac{dQ}{dn}\right)\left(1 - L_F + \frac{n}{2Q}\frac{dL_F}{dn}\right)\right. \\ &- \left.n\frac{dL_F}{dn}\left(1 - 2Q + \frac{n}{2Q^2}\frac{dQ}{dn}\right) + \frac{n^2}{2Q}\frac{d^2L_F}{dn^2}\right]. \end{aligned} \quad (39)$$

Similar considerations as with Eq. (36) hold for the ratio of the specific heats

$$\frac{C_P}{C_V} = 1 + \frac{8}{9}\frac{aQ^2T^2}{\frac{dP_0}{dn}}. \quad (40)$$

135 Other quantities of interest in astrophysical applications include the thermal index  $\Gamma_{th}$

$$\Gamma_{th} = 1 + \frac{P_{th}}{nE_{th}} = 1 + \frac{2Q}{3} - \frac{4}{5\pi^2}a^2nT^2\frac{dL_F}{dn} \quad (41)$$

and the adiabatic index  $\Gamma_S$

$$\Gamma_S = \frac{C_P}{C_V}\frac{n}{P}\frac{\partial P}{\partial n}\Big|_T = \frac{n}{P_0}\left[\frac{dP_0}{dn} + \frac{2}{3}aQT^2\left(1 + \frac{2Q}{3} + n\frac{dQ}{dn} - \frac{n}{P_0}\frac{dP_0}{dn}\right)\right] \quad (42)$$

where, in addition to Eqs. (34),(39) and (40), the approximation

$$\frac{1}{P} \simeq \frac{1}{P_0}\left(1 - \frac{P_{th}}{P_0}\right) \quad (43)$$

was used. In its native variables  $(n, S)$ ,  $\Gamma_S$  is given by

$$\Gamma_S = \frac{n}{P}\frac{\partial P}{\partial n}\Big|_S = \frac{n}{P_0 + \frac{nQS^2}{6a}}\left[\frac{dP_0}{dn} + \frac{QS^2}{6a}\left(1 + \frac{2}{3}Q + \frac{n}{Q}\frac{dQ}{dn}\right)\right]. \quad (44)$$

140 To arrive to Eq. (44) one begins by inverting Eq. (32) for the small parameter

$$aT = \frac{S}{2} + \frac{S^3}{5\pi^2}(1 - L_F) \quad (45)$$

which is then employed in the expression for the thermal pressure with the results

$$\begin{aligned} P_{th} &= \frac{nQ}{6a}S^2 + \frac{nQ}{30\pi^2a}S^4\left(1 - L_F - \frac{3n}{2Q}\frac{dL_F}{dn}\right) \\ \frac{\partial P_{th}}{\partial n}\Big|_S &= \frac{Q}{6a}S^2\left(1 + \frac{2}{3}Q + \frac{n}{Q}\frac{dQ}{dn}\right) \end{aligned} \quad (46)$$



$$\begin{aligned}
& + \frac{Q}{30\pi^2 a} S^4 \left[ \left( 1 + \frac{2}{3} Q + \frac{n}{Q} \frac{dQ}{dn} \right) (1 - L_F) \right. \\
& \left. - 2n \frac{dL_F}{dn} \left( 1 + \frac{3}{2Q} \right) - \frac{3n^2}{2Q} \frac{d^2 L_F}{dn^2} \right]. \quad (47)
\end{aligned}$$

Finally, the result is truncated to  $\mathcal{O}(S^2)$  in both the numerator as well as the denominator. We refrain from invoking approximation (43) as for nuclear systems,  $P_0$  can cross 0 at low densities. This is not a problem in the variables  $(n, T)$  because the degenerate approximation breaks down at sufficiently low density regardless of  $T$ . In the variables  $(n, S)$ , however, for small values of the entropy the system remains degenerate irrespective of the density, and thus division by zero is avoided (as could happen if Eq. (43) is used).

We point out that the adiabatic index is related to the squared speed of sound  $c_s$  according to

$$\left( \frac{c_s}{c} \right)^2 = \Gamma_S \frac{P}{h + mn}, \quad (48)$$

where  $h = nE + P$  is the enthalpy density.

#### 4. RESULTS FOR D=2

In condensed matter physics, 2-dimensional systems are of much interest. In the current framework, the entropy density is

$$s = \frac{\pi^2}{3} C_2 m^* T + \frac{7\pi^4}{90} C_2 \frac{m^{*3} T^3}{p_F^4} \left( p_F^2 \frac{\mathcal{M}_F'^2}{m^{*2}} + p_F^2 \frac{\mathcal{M}_F''}{m^*} - p_F \frac{\mathcal{M}_F'}{m^*} \right) \quad (49)$$

with  $C_2 = (1/2\pi\hbar^2)$ . A noteworthy feature of this result is that the  $\mathcal{O}(T^3)$  term receives contributions only from the derivatives of the effective mass function with respect to  $p$  at the Fermi surface. Thus, it is absent not only for free gases but also for systems with contact interactions where the  $p^2$ -dependence of  $R$  implies that  $d\mathcal{M}/dp = 0$ .

In terms of the level density parameter  $a = \pi^2 m^* / (2p_F^2)$ , and

$$p_F = \left( \frac{2n}{C_2} \right)^{1/2}, \quad Q = 1 - \frac{n}{m^*} \frac{dm^*}{dn} \quad (50)$$

$$L_F = p_F^2 \frac{\mathcal{M}_F'^2}{m^{*2}} + p_F^2 \frac{\mathcal{M}_F''}{m^*} - p_F \frac{\mathcal{M}_F'}{m^*} \quad (51)$$

Eq. (49) leads to

$$S = \frac{4}{3} a T + \frac{56}{45\pi^2} a^3 T^3 L_F, \quad E_{th} = \frac{2}{3} a T^2 + \frac{14}{15\pi^2} a^3 T^4 L_F \quad (52)$$

$$P_{th} = \frac{2}{3} a n Q T^2 + \frac{14}{15\pi^2} a^3 n Q T^4 \left( L_F - \frac{n}{3Q} \frac{dL_F}{dn} \right) \quad (53)$$

$$\mu_{th} = -\frac{2}{3} a T^2 (1 - Q) - \frac{14}{45\pi^2} a^3 T^4 \left[ L_F (1 - 3Q) + n \frac{dL_F}{dn} \right] \quad (54)$$

$$C_V = \frac{4}{3} a T + \frac{56}{15\pi^2} a^3 T^3 L_F \quad \text{and} \quad C_P = C_V + \frac{16}{9} \frac{a^2 Q^2 T^3}{\frac{dP_0}{dn}}. \quad (55)$$

The above results do not include the effects of collective excitations near the Fermi surface or of non-analytic contributions. As pointed out in Ref. [9], 2-dimensional Fermi systems in condensed matter physics (even with contact interactions) have  $T^2$  contributions to the entropy from interactions separate from those due to the collective modes. These  $T^2$  contributions arise from non-analytic corrections to the real part of the self-energy.

## 5. APPLICATION TO MODELS

In what follows, we compare the analytical results from the leading order corrections to Landau Fermi-liquid theory to the results of exact numerical calculations of the thermal state variables. These comparisons are made using models that are widely used in nuclear and neutron star phenomenology. In the category of non-relativistic potential models, we begin with the model, referred to as MDI(A), that reproduces the empirical properties of isospin symmetric and asymmetric bulk nuclear matter [10], optical model fits to nucleon-nucleus scattering data [11], heavy-ion flow data in the energy range 0.5-2 GeV/A [12], and the largest well-measured neutron star mass of  $2 M_\odot$  [13, 14]. This model, which is based on Refs. [15, 16], incorporates finite range interactions through a Yukawa-type, finite-range force, is contrasted with a conventional zero-range Skyrme model known as SkO' [17]. Both models predict nearly identical zero-temperature properties at all densities and proton fractions, including the neutron star maximum mass, but differ in their predictions for heavy-ion flow data [18]. To provide a contrast, we also investigate a relativistic mean-field theoretical (MFT) model [10] which yields zero-temperature properties similar to those of the two non-relativistic models chosen here. For all three models, we consider nucleonic matter in its pure neutron-matter (PNM, with  $\gamma = 2$ ) and symmetric nuclear matter (SNM, with  $\gamma = 4$ ) configurations.

### 5.1. Finite-range potential models

For the MDI(A) model [16, 10], the momentum-dependent part of the single-particle potential is given by

$$R(p) = \frac{2C_\gamma}{n_0} \frac{2}{(2\pi\hbar)^3} \int d^3p' f_{p'} \frac{1}{1 + \left(\frac{\vec{p}-\vec{p}'}{\Lambda}\right)^2} \quad (56)$$

$$\begin{aligned} \xrightarrow{T=0} & \frac{C_\gamma}{n_0} \frac{\Lambda^3}{\pi^2 \hbar^3} \left\{ \frac{p_F}{\Lambda} - \arctan\left(\frac{p+p_F}{\Lambda}\right) + \arctan\left(\frac{p-p_F}{\Lambda}\right) \right. \\ & \left. + \frac{(\Lambda^2 + p_F^2 - p^2)}{4\Lambda p} \ln \left[ \frac{\Lambda^2 + (p+p_F)^2}{\Lambda^2 + (p-p_F)^2} \right] \right\}. \end{aligned} \quad (57)$$

For the coefficients  $n_0$ ,  $C_2$ ,  $C_4$  and  $\Lambda$  we use the values  $0.16 \text{ fm}^{-3}$ ,  $-23.06 \text{ MeV}$ ,  $-128.9 \text{ MeV}$  and  $420.9 \text{ MeV}$ , respectively. Explicit expressions for the derivatives of  $R(p)$  and their connection with  $\mathcal{M}$  and  $L_F$  are provided in Appendix A. The MDI Hamiltonian density is shown in Appendix B. For details of the exact numerical calculations, see Ref. [10].

### 5.2. Zero-range Skyrme models

Zero-range Skyrme models belong to that subset of the  $D = 3$  case for which  $L_F = 0$ . This is because, for these models, the momentum-dependent part of the potential has the form

$$R = \beta(n)p^2 \quad (58)$$

( $\beta(n)$  is a density dependent factor) which renders the generalized effective mass to be  $p$ -independent:

$$\mathcal{M} = \frac{m}{1 + \frac{m}{p} \frac{dR}{dp}} = \frac{1}{1 + 2m\beta(n)}, \quad (59)$$

and therefore its derivatives  $\mathcal{M}' = \mathcal{M}'' = 0$ . Hence  $L_F = 0$  as well. Consequently, the results in Sec. 3 for Skyrme models simplify considerably. Results to be shown here are for the SKO' model [17], the exact numerical calculations for which are described in Ref. [10].

### 5.3. Relativistic models

The single-particle energy spectrum of relativistic mean-field theoretical models [19] obtained from the nucleon equation of motion has the structure

$$\epsilon = E^* + U(n), \quad E^* = [p^2 + M^{*2}(n, T)]^{1/2}. \quad (60)$$

The single-particle potential  $U(n)$  is the result of vector meson exchanges whereas the Dirac effective mass  $M^*$  arises from scalar meson interactions. The implementation of the above equations in the Sommerfeld expansion is made possible by the identification

$$y = \frac{E^*}{T}, \quad \frac{dy}{dp} = \frac{p}{E^*T} \quad \text{and} \quad \phi(y) = \frac{E^*T}{p} g(p). \quad (61)$$

The calculation of  $d\phi/dy$ ,  $d^3\phi/dy^3$  and  $n$  proceeds as in the non-relativistic case with the replacement  $\mathcal{M} \rightarrow E^*$  [cf. Eq. (8)]. In particular, for  $p_\mu$  we have

$$p_\mu = p_F \left[ 1 - \frac{\pi^2}{6} \frac{E_F^{*2} T^2}{p_F^4} \left( D - 2 + \frac{p_F E_F'^*}{E_F^*} \right) \right] \quad (62)$$

where

$$E_F^* = (p_F^2 + M^{*2})^{1/2} \quad \text{and} \quad E_F'^* = \left. \frac{dE^*}{dp} \right|_{p_F} = \frac{p_F}{E_F^*}. \quad (63)$$

The simple dependence of  $E^*$  on the momentum  $p$  in Eq. (60) leads to the correspondingly straightforward expression (63) for  $E_F'^*$  which, as we will show soon hereafter, results in an elementary form for  $L_F$  and by extension the whole set of the MFT thermodynamics can be written in an uncomplicated manner.

Substituting Eq. (63) into Eq. (62) yields

$$p_\mu = p_F \left[ 1 - \frac{\pi^2}{6} \frac{E_F^{*2} T^2}{p_F^4} \left( D - 2 + \frac{p_F^2}{E_F^{*2}} \right) \right]. \quad (64)$$

The twice-by-parts integration of Eq. (17) for the entropy density in the relativistic context gives

$$s = \frac{C_D}{T} \int dp p^{D-1} f_p \left( E^* + \frac{p}{D} \frac{dE^*}{dp} - E_\mu^* \right) \quad (65)$$

where one observes the analogy with the integral term of Eq. (20). Using

$$g_s(p) = p^{D-1} \left( E^* + \frac{p}{D} \frac{dE^*}{dp} - E_\mu^* \right) \quad (66)$$

225 we proceed as before to get the entropy density in terms of  $p_\mu$  as

$$s = \frac{\pi^2}{3} C_D p_\mu^{D-2} E_\mu^* T + \frac{7\pi^2}{90} C_D (D-2)(D-4) p_\mu^{D-6} E_\mu^{*3} T^3 \left[ 1 + \frac{3}{(D-4)} \frac{p_\mu^2}{E_\mu^{*2}} \right] \quad (67)$$

which, with the aid of Eq. (62), becomes

$$\begin{aligned} s &= \frac{\pi^2}{3} C_D p_F^{D-2} E_F^* T + \frac{\pi^4}{45} C_D (D-2)(D-9) p_F^{D-6} E_F^{*3} T^3 \\ &\times \left[ 1 + \frac{11}{2(D-9)} \frac{p_F^2}{E_F^{*2}} - \frac{5}{2(D-2)(D-9)} \frac{p_F^4}{E_F^{*4}} \right]. \end{aligned} \quad (68)$$

In the derivation of the last equation the weak temperature of  $M^*$  in the degenerate limit has been ignored (but not of  $E_\mu^*$ ). Combining Eq. (68) with Eqs. (25)-(27) in  $D=3$ , and using the definitions [here, the Fermi temperature 230  $T_F = p_F^2/(2E_F^*)]$

$$a = \frac{\pi^2}{2} \frac{E_F^*}{p_F^2}, \quad q = \frac{M^{*2}}{E_F^{*2}} \left( 1 - \frac{3n}{M^*} \frac{dM^*}{dn} \right) \quad \text{and} \quad L_F = \frac{11}{12} \frac{p_F^2}{E_F^{*2}} - \frac{5}{12} \frac{p_F^4}{E_F^{*4}}, \quad (69)$$

we obtain

$$S = 2aT - \frac{16}{5\pi^2} a^3 T^3 (1 - L_F), \quad E_{th} = aT^2 - \frac{12}{5\pi^2} a^3 T^4 (1 - L_F) \quad (70)$$

$$P_{th} = \frac{1}{3} a n T^2 (1 + q) - \frac{4}{5\pi^2} a^3 n T^4 \left[ 1 - L_F + q \left( 1 - \frac{L_F}{3} - \frac{10}{9} \frac{p_F^4}{E_F^{*4}} \right) \right] \quad (71)$$

$$\mu_{th} = -\frac{2}{3} a T^2 \left( 1 - \frac{q}{2} \right) - \frac{4}{5\pi^2} a^3 T^4 q \left( 1 - \frac{L_F}{3} - \frac{10}{9} \frac{p_F^4}{E_F^{*4}} \right) \quad (72)$$

$$C_V = 2aT - \frac{48}{5\pi^2} a^3 T^3 (1 - L_F) \quad \text{and} \quad C_P = C_V + \frac{4}{9} \frac{a^2 T^3 (1 + q)^2}{\frac{dP_0}{dn}}. \quad (73)$$

As in the nonrelativistic case, when conditions are such that  $dP_0/dn$  is small, one must use derivatives of the pressure with respect to  $n$  and  $T$  that include thermal contributions to  $\mathcal{O}(T^4)$  in the calculation of  $C_P$ . Explicitly,

$$\left( \frac{\partial P_{th}}{\partial T} \Big|_n \right)^2 = \frac{4}{9} a^2 n^2 T^2 (1 + q)^2$$

$$\begin{aligned}
& \times \left\{ 1 - \frac{48}{5\pi^2} \frac{a^2 T^2}{1+q} \left[ 1 - L_F + q \left( 1 - \frac{L_F}{3} - \frac{10}{9} \frac{p_F^4}{E_F^{*4}} \right) \right] \right\} \quad (74) \\
\frac{\partial P}{\partial n} \Big|_T &= \frac{dP_0}{dn} + \frac{T^2 a}{9} \left[ (1+q)(2-q) + 3n \frac{dq}{dn} \right] \\
&+ \frac{4}{5\pi^2} T^4 a^3 q \left[ 1 - L_F + \left( q - \frac{n}{q} \frac{dq}{dn} \right) \left( 1 - \frac{L_F}{3} - \frac{10}{9} \frac{p_F^4}{E_F^{*4}} \right) \right] \\
&+ \frac{n}{q} \frac{dL_F}{dn} \left( 1 + \frac{q}{3} \right) + \frac{40}{27} \frac{p_F^4}{E_F^{*4}} q \quad (75) \\
\frac{dq}{dn} &= -\frac{2}{3n} q(1-q) + \frac{1}{M^*} \frac{dM^*}{dn} q - \frac{M^*}{2E_F^{*2}} \left( \frac{dM^*}{dn} + \frac{3n}{2} \frac{d^2 M^*}{dn^2} \right) \quad (76)
\end{aligned}$$

## 235 6. RESULTS AND DISCUSSION

Here, we compare the results from FLT and FLT+NLO with the exact numerical results for the two non-relativistic models (MDI(A) and SkO'), and for a relativistic mean-field theoretical model (MFT). Numerical techniques for obtaining the exact numerical results are detailed in Refs. [20, 21]. The thermal properties presented for PNM and SNM are at a temperature of  $T = 20$  MeV.

In the top panels of Fig. 1, the Landau effective masses  $m_n^*$  of the neutron scaled with its vacuum value are shown as a function of baryon density  $n$ . For the MFT model, both  $m_n^* = E_{F_n}^* = \sqrt{M^{*2} + k_{F_n}^2}$  and the Dirac effective mass  $M^*$  are shown. Noteworthy points for the non-relativistic models are: (i) The isospin splittings are qualitatively similar -  $m_n^*/m$  being larger for PNM than for SNM - although quantitative differences are present, and (ii) except for  $n$  up to  $0.2 \text{ fm}^{-3}$ , the decrease with increasing  $n$  for the MDI model is relatively slow (logarithmic decline) compared with that for the SkO' model  $[(1 + \beta n)^{-1} \text{ fall off}]$ . This overall flatness of  $m^*$  for the MDI model is a direct consequence of the momentum structure of its single-particle potential which causes it to saturate at high momenta. For the MFT model,  $M^*$  decreases monotonically with  $n$  to values lower than those for the non-relativistic models. The Landau mass  $m^*$ , however, exhibits a non-monotonic behavior, attaining a minimum for  $n_{min} = 0.57 \text{ (0.52) fm}^{-3}$  obtained from the solution of

$$\frac{p_F}{M^*} + \frac{dM^*}{dp_F} = 0 \quad (77)$$

for the case of SNM (PNM), and increasing thereafter due to the monotonic increase of  $k_{F_n}$  with  $n$ . Physically,  $n_{min}$  marks the transition of nucleons well into the relativistic region. The density  $n_R$  at which  $p_F = M^*$  occurs at

$$n_R = 0.643 \gamma \left( \frac{M^*}{m} \right)^3 \text{ fm}^{-3} \quad (78)$$

about  $(2/3) n_{min} = 0.38$  (0.34)  $\text{fm}^{-3}$  for SNM (PNM) which signals the onset of relativistic effects which become progressively important for  $n \geq n_R$ .

The bottom panels of Fig. 1 show the logarithmic derivatives of  $m_n^*$  vs  $n$ . Also shown for the MFT model is  $d \ln M^* / d \ln n$  which has been divided by a factor of 3 to fit within the figure. The logarithmic derivatives  $m^*$  for MDI(A) show little variation with  $n$  at supra-nuclear densities. In contrast, results for the SkO' model, which take the simple form  $(m_n^*/m) - 1$ , show a significant variation with  $n$ . The logarithmic derivative of  $M^*$  in MFT drops to values considerably lower than for the other two models. This derivative remains negative but approaches a constant value at large densities. The logarithmic derivative of the Landau effective mass drops until  $\sim 2n_0$ , but then increases to positive values. This behavior is a reflection of the minimum that occurs for  $m_n^*$  in this model. As will be seen below, the density dependences of the effective masses and their logarithmic derivatives determine the behavior of all the thermal properties in FLT. Higher order derivatives of the Landau effective mass function in Eq. (8) appear in FLT+NLO.

The FLT and FLT+NLO results for the thermal energy,  $E_{th}$  vs  $n$ , are compared with the exact numerical results in Fig. 2. The NLO corrections to FLT yield agreement with the exact results down to sub-nuclear densities of 0.5 to 1  $n_0$  compared to 2-3  $n_0$  for FLT. As is the case with FLT, slightly but systematically better agreement with FLT+NLO occurs for PNM than for SNM for all the thermodynamic quantities we study. This is a consequence of the fact that the neutron density in PNM ( $n_n = n$ ) is twice the neutron density in SNM ( $n_n = n/2$ ); PNM is more degenerate than SNM at the same baryon density  $n$ .

In Figure 3, we show the convergence of FLT and FLT+NLO results to the exact numerical results for  $P_{th}$ . For all three models, the FLT+NLO results extend the agreement with the exact results to lower densities than those of FLT. The SkO' model shows the greatest changes relative to FLT for both SNM and PNM. Both the MDI(A) and MFT results also show improvement using FLT+NLO with better agreement occurring for PNM. For  $P_{th}$  at  $n > n_0$ , the influence of  $m^*(n)$  and its logarithmic derivative with respect to  $n$  (in FLT), and the higher derivatives of  $\mathcal{M}$  (in FLT+NLO) are amply demonstrated: (i) for MDI(A),  $P_{th}$  grows very slowly with  $n$ ; (ii) considerably larger growth with  $n$  is exhibited for SkO' than for MDI(A); and (iii) for MFT, the prominent peaks in  $P_{th}$  at intermediate densities are due to the minima in  $m^*$  and  $d \ln M^* / d \ln n$  at similar densities. For asymptotic densities,  $P_{th} \propto n^{4/3}$  in MFT models characteristic of massless particles. A corresponding behavior is also present in the thermal chemical potentials (see below).

Comparisons of the entropy per baryon,  $S$ , are shown in Fig. 4. For all three models, the agreement between the exact results and those of FLT+NLO extends to below  $n_0$ , and to as low as  $n_0/4$  for PNM with MFT. This is an improvement from the FLT results for which convergence ranged from  $1.5n_0$

305 (FLT and PNM) to  $3n_0$  (SkO' and SNM).

In Fig. 5, the thermal parts of the neutron chemical potentials,  $\mu_{n,th}$ , are shown as a function of  $n$ . Results from FLT+NLO lie closer to the exact results than do those of FLT with the agreement extending to sub-nuclear densities. As  
 310 with the other state variables, the agreement is quantitatively better for PNM than for SNM.

The specific heat at constant volume,  $C_V$ , is presented in Fig. 6 as a function of  $n$ . For all models, the FLT+NLO results show better agreement with  
 315 the exact results than those of FLT. The lowest density for which the agreement extends differs between the models, that for the SkO' model being higher than for the other two models particularly for SNM.

In Figure 7 we show the specific heat at constant pressure and its limiting  
 320 cases as functions of  $n$ . The maxima at low sub-nuclear densities in the exact numerical results are related to the liquid-gas phase transition of nucleonic matter which occurs at  $T \sim 15$ -20 MeV. The convergence between the exact and approximate results for MDI(A) and MFT follows a pattern similar to the quantities discussed previously with the conspicuous exception of FLT which  
 325 appears to outperform FLT+NLO for SNM. We attribute this feature to a numerical accident, possibly due to the proximity to the phase transition. Note that FLT begins to deviate from the exact result for densities below  $n \sim 3n_0$  in the case of SkO'. As our analysis here is concerned with the degenerate region, this failure at sub-nuclear densities is not surprising. For an adequate treatment  
 330 in the non-degenerate region, see Ref. [10].

The thermal index,  $\Gamma_{th} = 1 + (P_{th}/\varepsilon_{th})$ , is shown in Fig. 8. For the SkO' model, the FLT result is exact for all regions of degeneracy. This happenstance is due to the fact that for non-relativistic nucleons with only contact interactions,  
 335  $P_{th}$  and  $\varepsilon_{th}$  can be written entirely in terms of their ideal-gas counterparts as

$$\begin{aligned} P_{th}(n, T) &= P_{th}^{id}(n, T; m^*) Q \\ \varepsilon_{th}(n, T) &= \varepsilon_{th}^{id}(n, T; m^*), \quad \frac{P_{th}^{id}}{\varepsilon_{th}^{id}} = \frac{2}{3} \end{aligned} \quad (79)$$

regardless of the degree of degeneracy. The  $n$ -dependence of  $m^*$  for Skyrme-like interactions thus yields

$$\Gamma_{th} = \frac{8}{3} - \frac{m^*(n)}{m}. \quad (80)$$

For the finite-range MDI(A) and the relativistic MFT models, the FLT+NLO results mildly improve the FLT results in reproducing the exact ones. This  
 340 marginal improvement is related to the ratio  $P_{th}/\varepsilon_{th}$  in  $\Gamma_{th}$  in these cases, which amount to a constant plus a correction due to effects of  $n$  plus a second correction due to  $(n, T)$  effects, which means that temperature effects are sub-leading, and therefore very weak. Note that the results for the three models

differ significantly from each other, both qualitatively and quantitatively. These  
 345 differences are due to the differences in the effective mass functions of the models.

In physical applications involving neutron stars and supernovae, contribu-  
 tions from leptons (electrons and muons) and photons must be included to all of  
 the state variables. Thermal effects from these sources are adequately given by  
 their free gas forms, and numerical methods for their calculation for arbitrary  
 350 degeneracy can be found in Ref. [20]. The influence of thermal effects from  
 leptons and photons to the total has been detailed in Ref. [10], and will not be  
 repeated here.

## 7. SUMMARY AND CONCLUSIONS

For homogeneous systems of fermions in the limit of extreme degeneracy  
 355 ( $T/T_F \ll 1$ , where  $T_F$  is the Fermi temperature), Landau's Fermi Liquid The-  
 ory (FLT) provides simple analytical expressions that are model independent  
 for the thermal state variables (*e.g.*, entropy, energy, pressure, chemical poten-  
 tial, and specific heats) [1]. In the absence of collective excitations close to the  
 Fermi surface, thermal effects are primarily determined by the nucleon's Lan-  
 360 dau effective mass and its first density derivative which in turn depend on the  
 momentum-dependence of the  $T = 0$  single-particle energy spectrum.

In this work, we have developed a method by which thermal effects in near-  
 degenerate to degenerate matter can be described to next-to-leading order in  
 $T/T_F$  for models with general momentum dependences in their single-particle  
 365 potentials. Analytical formulas valid to next-to-leading order in  $T/T_F$  for all  
 of the thermal state variables are presented. The entropy density and spe-  
 cific heats are carried to  $\mathcal{O}(T/T_F)^3$  whereas the energy density and pressure  
 to  $\mathcal{O}(T/T_F)^4$ , extending the leading order results of FLT. These extensions in-  
 volved the use of a generalized Landau effective mass function which enables  
 370 the calculation of the entropy density, and thereafter the other state variables,  
 for a general single-particle spectrum. In special cases, *e.g.*, models with con-  
 tact interactions, knowledge of the Landau effective mass suffices. In the case  
 of finite-range interactions, momentum derivatives of the Landau effective mass  
 function up to second order are required to satisfy the thermodynamic identity.  
 375 Our results are valid for potential and field-theoretical models as long as the un-  
 derlying interactions yield a single-particle spectrum that is weakly dependent  
 on temperature in the degenerate limit.

We find that  $\mathcal{O}(T^3)$  corrections in 2-dimensions for non-relativistic models  
 appear only if they include finite-range interactions or, equivalently, if the mo-  
 380 mentum content of their mean field is something other than quadratic. These  
 contributions supplement the  $\mathcal{O}(T^2)$  non-analytic contributions even with zero-  
 range interactions established previously [9].

To illustrate the density region of their applicability, numerical results from  
 the new formulas were compared with those of exact numerical calculations  
 385 for zero- and finite-range potential models as well as for relativistic mean-field  
 theoretical (MFT) models widely used in astrophysical applications of hot and  
 dense nuclear matter. In all cases, excellent agreement with the exact results



390 was found even to sub-nuclear densities of  $\sim 0.1 \text{ fm}^{-3}$  for  $T = 20 \text{ MeV}$ , whereas  
 FLT results are valid only for densities beyond  $\sim 0.3 \text{ fm}^{-3}$ . (For low tempera-  
 395 tures and below  $\sim 0.1 \text{ fm}^{-3}$ , inhomogeneous phases with nuclei and pasta-like  
 configurations are known to exist, and must be treated separately.) In addition  
 to providing physical insights, our analytical results facilitate a rapid evaluation  
 of the EOS in the homogeneous phase (important for computer-time consuming  
 large-scale simulations of supernovae, proto-neutron stars, and mergers of binary  
 395 compact objects). Our formulas can be used for any  $T = 0$  quasi-particle spec-  
 trum, *e.g.*, those extracted from Brueckner-Hartree-Fock and Dirac-Brueckner-  
 Hartree-Fock approaches, extensions of MFT models with non-linear derivatives  
 or with 2-loop effects, and effective field-theoretical approaches.

400 Examples of contributions not included in our work arise from, *e.g.*, non-  
 analytic contributions from single particle-hole excitations and, collective and  
 paring correlations close to the Fermi surface. Their roles as functions of den-  
 sities and temperatures of relevance to astrophysical phenomena need further  
 investigation.

## ACKNOWLEDGEMENTS

405 This work was supported by the U.S. DOE under Grants No. DE-FG02-  
 93ER-40756 and No. DE-FG02-87ER-40317.

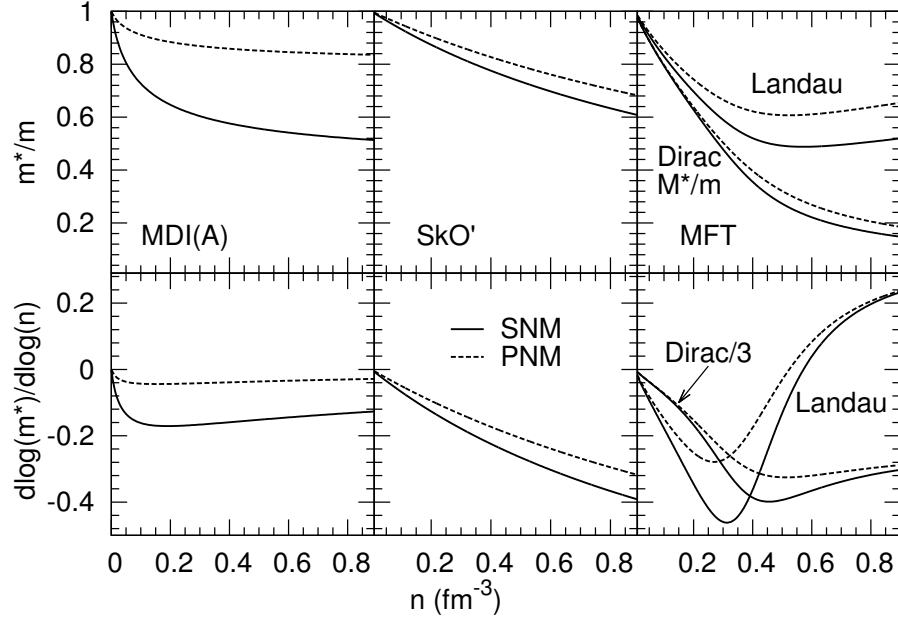


Figure 1: Top panels: Effective mass vs density for non-relativistic potential models (MDI(a) and SkO') and relativistic mean-field theoretical model (MFT) for symmetric nuclear matter (SNM) and pure neutron matter (PNM). Bottom panels: Logarithmic derivative of the effective mass with respect to density vs density.

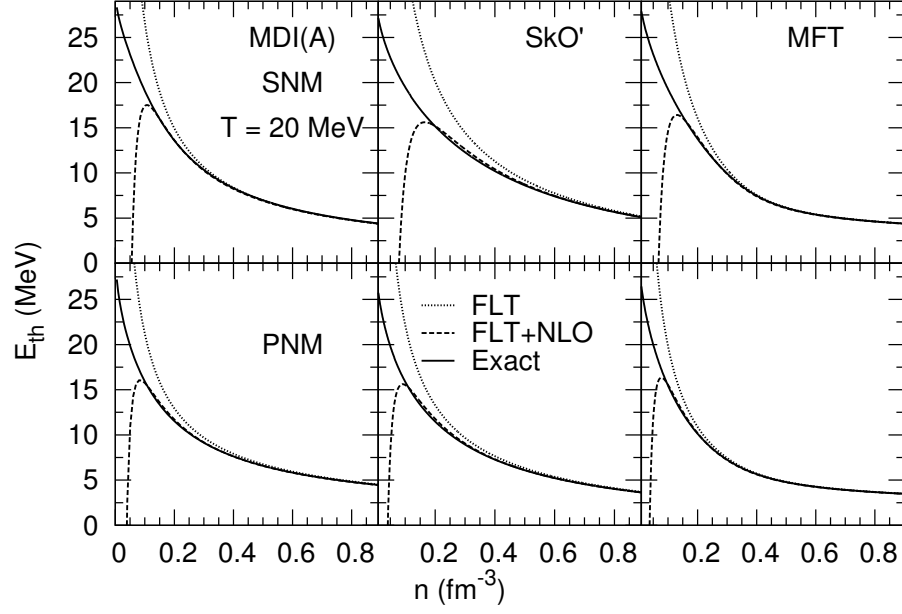


Figure 2: Thermal energy vs baryon density for the three models at a temperature of  $T = 20$  MeV. Results for SNM are in the top panels and for PNM in the bottom panels.

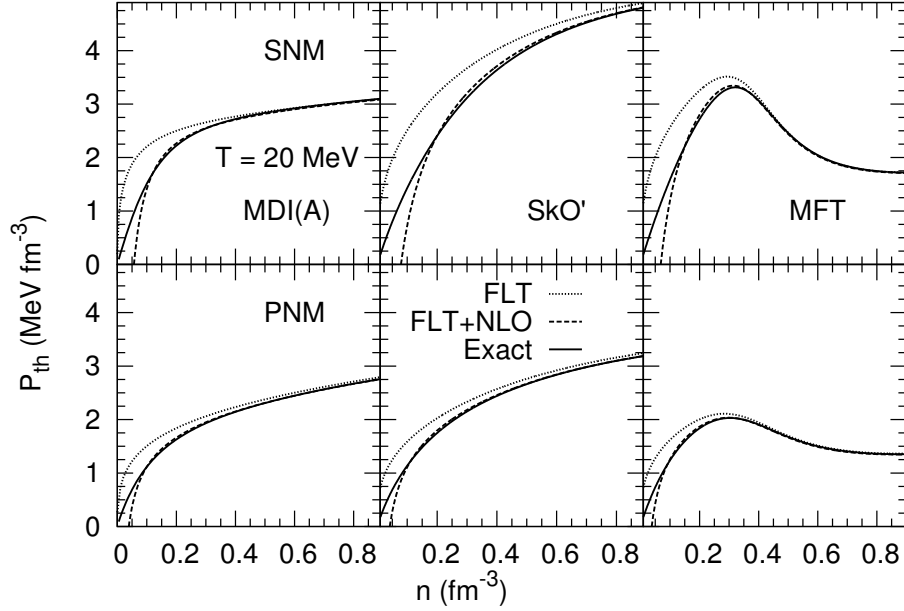


Figure 3: Same as Fig. 2, but for thermal pressure.

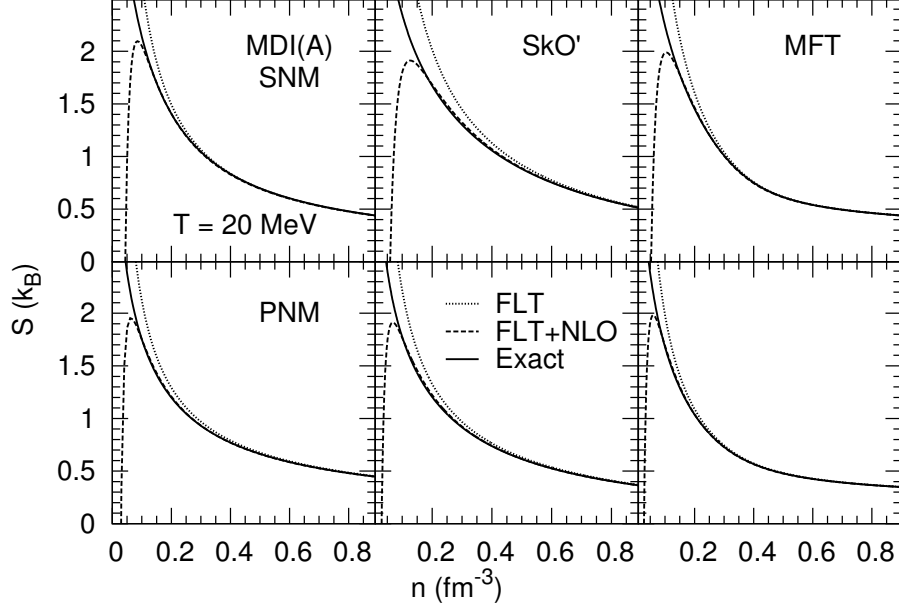


Figure 4: Same as Fig. 2, but for entropy per baryon.

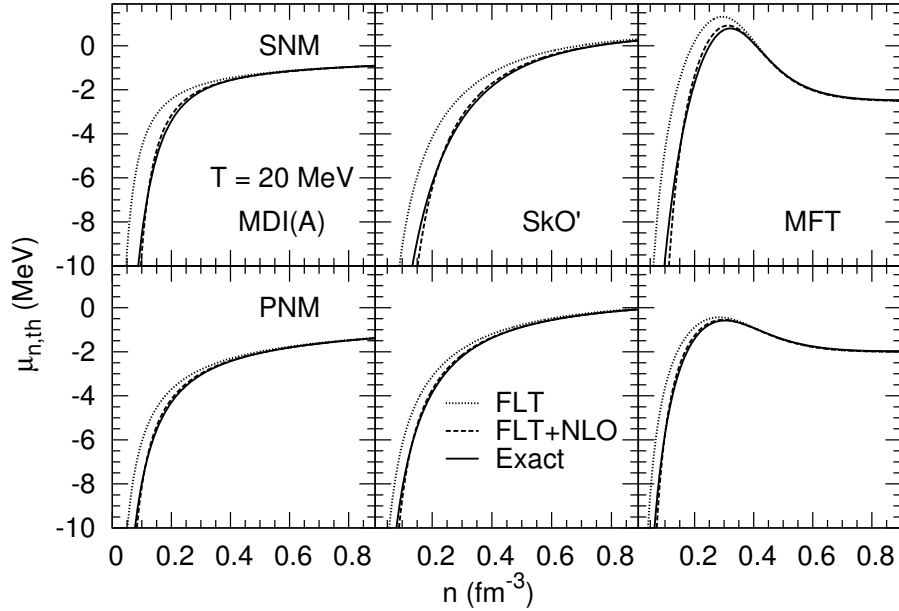


Figure 5: Same as Fig. 2, but for thermal neutron chemical potential.

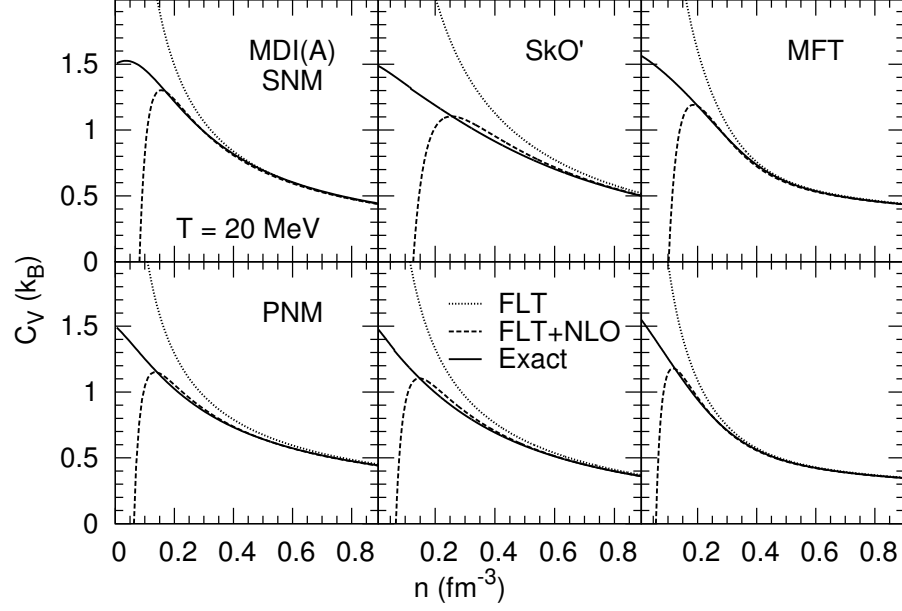


Figure 6: Same as Fig. 2, but for specific heat at constant volume.

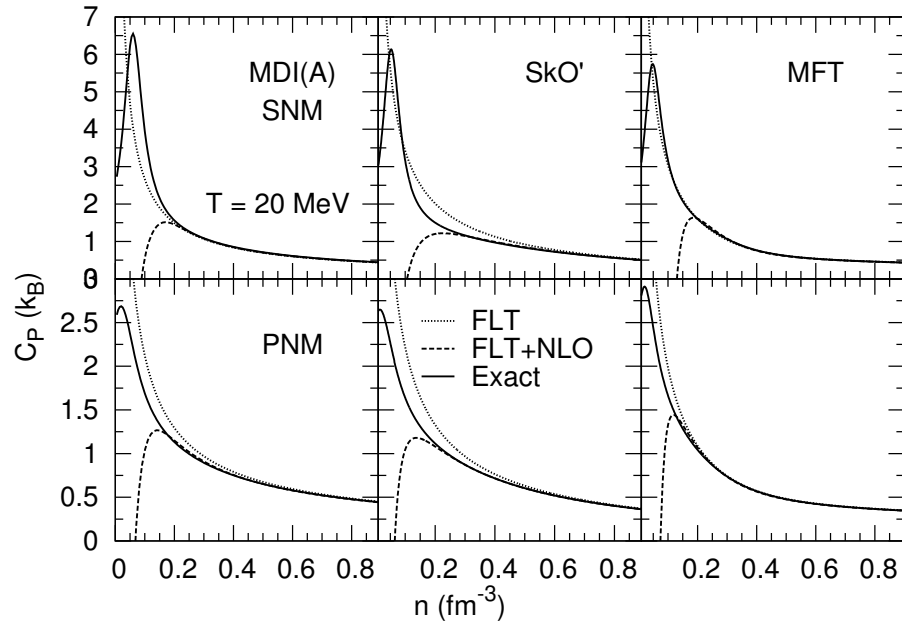


Figure 7: Same as Fig. 2, but for specific heat at constant pressure.

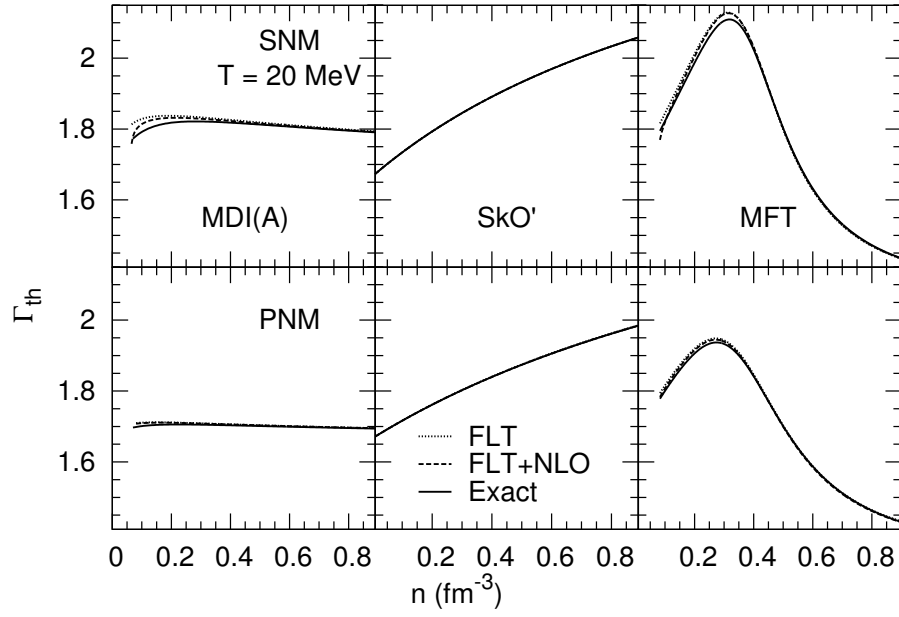


Figure 8: Same as Fig. 2, but for the thermal index.

## Appendix A. RESULTS RELATED TO $L_F$

Here we collect relations required to calculate the quantity  $L_F$  defined in Eq. (29) of Sec. 3.

410 *Model-independent relations*

$$\mathcal{M}' \equiv \frac{d\mathcal{M}}{dp} = \frac{\mathcal{M}^2}{p^2} \left( \frac{dR}{dp} - p \frac{d^2 R}{dp^2} \right) \quad (\text{A.1})$$

$$\mathcal{M}'' = \frac{2\mathcal{M}^3}{p^4} \left( \frac{dR}{dp} - p \frac{d^2 R}{dp^2} \right) - \frac{2\mathcal{M}^2}{p^3} \left( \frac{dR}{dp} - p \frac{d^2 R}{dp^2} + \frac{p^2}{2} \frac{d^3 R}{dp^3} \right) \quad (\text{A.2})$$

$$= -2 \frac{\mathcal{M}'}{p} \left( 1 - \frac{\mathcal{M}}{p} \right) - \frac{\mathcal{M}^2}{p} \frac{d^3 R}{dp^3} \equiv \frac{d^2 \mathcal{M}}{dp^2} \quad (\text{A.3})$$

$$\frac{dL_F}{dn} = \frac{p_F}{3n} \frac{dL_F}{dp_F} \quad (\text{A.4})$$

$$\begin{aligned} \frac{dL_F}{dp_F} &= \frac{5}{12} \frac{\mathcal{M}'_F}{m^*} \left( 1 - p_F \frac{\mathcal{M}'_F}{m^*} \right) \left( 1 - \frac{42}{5} p_F \frac{\mathcal{M}'_F}{m^*} \right) \\ &\quad - \frac{m^*}{6} \frac{d^3 R}{dp^3} \Big|_{p_F} \left( 1 + \frac{49}{2} p_F \frac{\mathcal{M}'_F}{m^*} \right) - \frac{7}{12} p_F m^* \frac{d}{dp_F} \frac{d^3 R}{dp^3} \Big|_{p_F} \end{aligned} \quad (\text{A.5})$$

The subscript  $F$  denotes evaluation at  $p = p_F$ .

*MDI model-specific relations*

$$\frac{dR}{dp} \Big|_{p_F} = \frac{C_\gamma}{n_0} \frac{\Lambda^2}{\pi^2 \hbar^3} \left[ 1 - \frac{1}{2} \left( 1 + \frac{\Lambda^2}{2p_F^2} \right) \ln \left( 1 + \frac{4p_F^2}{\Lambda^2} \right) \right] \quad (\text{A.6})$$

$$\begin{aligned} \frac{d^2 R}{dp^2} \Big|_{p_F} &= -\frac{2C_\gamma}{n_0} \frac{\Lambda^2}{\pi^2 \hbar^3} \frac{1}{p_F(4p_F^2 + \Lambda^2)} \left[ (3p_F^2 + \Lambda^2) \right. \\ &\quad \left. - (p_F^2 + \Lambda^2) \left( 1 + \frac{\Lambda^2}{4p_F^2} \right) \ln \left( 1 + \frac{4p_F^2}{\Lambda^2} \right) \right] \end{aligned} \quad (\text{A.7})$$

$$\begin{aligned} \frac{d^3 R}{dp^3} \Big|_{p_F} &= \frac{2C_\gamma}{n_0} \frac{1}{\pi^2 \hbar^3} \frac{1}{p_F^2(4p_F^2 + \Lambda^2)^2} \\ &\quad \times \left[ 8p_F^6 + 34p_F^4 \Lambda^2 + 21p_F^2 \Lambda^4 + 3\Lambda^6 \right. \\ &\quad \left. - \frac{3\Lambda^2}{4} \left( 1 + \frac{\Lambda^2}{p_F^2} \right) (4p_F^2 + \Lambda^2)^2 \ln \left( 1 + \frac{4p_F^2}{\Lambda^2} \right) \right] \end{aligned} \quad (\text{A.8})$$

$$\begin{aligned} \frac{d}{dp_F} \frac{d^3 R}{dp^3} \Big|_{p_F} &= -\frac{2C_\gamma}{n_0} \frac{1}{\pi^2 \hbar^3} \frac{1}{p_F^5(4p_F^2 + \Lambda^2)^3} \\ &\quad \times \left[ 4p_F^2(24p_F^8 + 134p_F^6 \Lambda^2 + 118p_F^4 \Lambda^4 + 33p_F^2 \Lambda^6 + 3\Lambda^8) \right. \\ &\quad \left. - 3\Lambda^2(p_F^2 + \Lambda^2)(4p_F^2 + \Lambda^2)^3 \ln \left( 1 + \frac{4p_F^2}{\Lambda^2} \right) \right] \end{aligned} \quad (\text{A.9})$$

## Appendix B. MDI HAMILTONIAN DENSITY

For the MDI models, the Hamiltonian density is composed of terms arising from kinetic sources,  $\mathcal{H}_k$ , density-dependent interactions,  $\mathcal{H}_d$ , and momentum-dependent interactions,  $\mathcal{H}_m$ :

$$\mathcal{H} = \mathcal{H}_k + \mathcal{H}_d + \mathcal{H}_m. \quad (\text{B.1})$$

At  $T = 0$ ,

$$\mathcal{H}_k = \frac{1}{2m}(\tau_n + \tau_p) = \frac{1}{2m} \frac{1}{5\pi^2 \hbar^3} (p_{Fn}^5 + p_{Fp}^5) \quad (\text{B.2})$$

$$\mathcal{H}_d = \frac{A_1}{2n_0} n^2 + \frac{A_2}{2n_0} n^2 (1 - 2x)^2 + \frac{B}{\sigma + 1} \frac{n^{\sigma+1}}{n_0^\sigma} [1 - y(1 - 2x)^2] \quad (\text{B.3})$$

$$\mathcal{H}_m = \frac{C_l}{n_0} (I_{nn} + I_{pp}) + \frac{2C_u}{n_0} I_{np} \quad (\text{B.4})$$

with

$$\begin{aligned} x &= n_p/n, \quad p_{Fi} = (3\pi^2 n_i \hbar^3)^{1/3} \\ I_{ij} &= \frac{8\pi^2 \Lambda^2}{(2\pi \hbar)^6} \left\{ p_{Fi} p_{Fj} (p_{Fi}^2 + p_{Fj}^2) - \frac{p_{Fi} p_{Fj} \Lambda^2}{3} \right. \\ &\quad + \frac{4\Lambda}{3} (p_{Fi}^3 - p_{Fj}^3) \arctan\left(\frac{p_{Fi} - p_{Fj}}{\Lambda}\right) \\ &\quad - \frac{4\Lambda}{3} (p_{Fi}^3 + p_{Fj}^3) \arctan\left(\frac{p_{Fi} + p_{Fj}}{\Lambda}\right) \\ &\quad + \left[ \frac{\Lambda^4}{12} + \frac{(p_{Fi}^2 + p_{Fj}^2) \Lambda^2}{2} - \frac{(p_{Fi}^2 - p_{Fj}^2)^2}{4} \right] \\ &\quad \times \left. \ln \left[ \frac{(p_{Fi} + p_{Fj})^2 + \Lambda^2}{(p_{Fi} - p_{Fj})^2 + \Lambda^2} \right] \right\}. \end{aligned} \quad (\text{B.6})$$

In this work we use the coefficients  $A_1 = -69.48$  MeV,  $A_2 = -29.22$  MeV,  $B = 100.1$  MeV,  $\sigma = 1.362$ ,  $y = -0.0328$ ,  $C_l = -23.06$  MeV,  $C_u = -105.9$  MeV, and  $\Lambda = 420.9$  MeV [10].

When a calculation for multiple-species is undertaken, highly asymmetric configurations should be avoided as the various particle types involved will be in different regimes of degeneracy thus resulting in a slower convergence relative to the single-species case. Furthermore, one should also refrain from using multiple species results with  $x = 0$  or  $1$  as numerical complications arise; namely, division by 0 occurs in the level density parameters  $a_i$ .

## Appendix C. MEAN-FIELD THEORETICAL MODEL (MFT)

The MFT model used here involves the exchange of  $\sigma$ ,  $\omega$  and  $\rho$  mesons (scalar, vector and iso-vector, respectively) [19]. Its Lagrangian density is

$$\mathcal{L} = \bar{\Psi} \left[ i\gamma_\mu \partial^\mu - \gamma_0 g_\omega \omega_0 - \gamma_0 \frac{g_\rho}{2} \rho_0 \tau_3 - (M - g_\sigma \sigma_0) \right] \Psi$$



$$- \frac{1}{2} \left[ m_\sigma^2 \sigma_0^2 + \frac{\kappa}{3} (g_\sigma \sigma_0)^3 + \frac{\lambda}{12} (g_\sigma \sigma_0)^4 \right] + \frac{1}{2} m_\omega^2 \omega_0^2 + \frac{1}{2} m_\rho^2 \rho_0^2 \quad (\text{C.1})$$

which yields the following meson equations of motion:

$$g_\sigma \langle \bar{\Psi} \Psi \rangle = g_\sigma n_S = m_\sigma^2 \sigma_0 + \frac{\kappa}{2} g_\sigma^3 \sigma_0^2 + \frac{\lambda}{6} g_\sigma^4 \sigma_0^3 \quad (\text{C.2})$$

$$\omega_0 = \frac{g_\omega}{m_\omega^2} \langle \Psi^\dagger \Psi \rangle = \frac{g_\omega}{m_\omega^2} n \quad (\text{C.3})$$

$$\rho_0 = \frac{g_\rho}{2m_\rho^2} \langle \Psi^\dagger \tau_3 \Psi \rangle = \frac{g_\rho}{2m_\rho^2} (n_n - n_p) \quad (\text{C.4})$$

in the mean-field approximation with classical expectation values denoted by the subscript “0”. The equation of motion for the nucleon ( $\Psi$ ) field is

$$\left[ i\gamma_\mu \partial^\mu - \gamma_0 (g_\omega \omega_0 + \frac{g_\rho}{2} \rho_0 \tau_3) - M^* \right] \Psi = 0 \quad (\text{C.5})$$

where  $M^* = M - g_\sigma \sigma_0$ , and yields the nucleon single-particle energy spectrum

$$\epsilon_{i\pm} = \pm E_i^* + \frac{g_\omega^2}{m_\omega^2} n + \frac{g_\rho^2}{4m_\rho^2} (n_i - n_j), \quad E_i^* = (p_i^2 + M^{*2})^{1/2}. \quad (\text{C.6})$$

435 The subscripts  $i, j$  refer to the nucleon species, the positive sign to the particles and the negative sign to the antiparticles. The thermodynamics of the system are obtained from its energy-momentum tensor

$$T_{\mu\nu} = \frac{\partial \mathcal{L}}{\partial (\partial_\mu \phi)} \partial_\nu \phi - g_{\mu\nu} \mathcal{L} \quad (\text{C.7})$$

$$= i\bar{\Psi} \gamma_\mu \partial_\nu \Psi + \frac{g_{\mu\nu}}{2} \left[ m_\sigma^2 \sigma_0^2 + \frac{\kappa}{3} (g_\sigma \sigma_0)^3 + \frac{\lambda}{12} (g_\sigma \sigma_0)^4 - m_\omega^2 \omega_0^2 - m_\rho^2 \rho_0^2 \right]. \quad (\text{C.8})$$

For an isotropic system in its rest-frame, the energy density and the pressure are given by the diagonal elements of  $T_{\mu\nu}$  as

$$\begin{aligned} \epsilon &= \langle T_{00} \rangle = 2 \sum_i \int f_{p_i} (p_i^2 + M^{*2})^{1/2} \frac{d^3 p_i}{(2\pi\hbar)^3} + \frac{g_\omega^2}{2m_\omega^2} n^2 \\ &+ \frac{g_\rho^2}{8m_\rho^2} (n_p - n_n)^2 + \frac{1}{2} \left[ m_\sigma^2 \sigma_0^2 + \frac{\kappa}{3} (g_\sigma \sigma_0)^3 + \frac{\lambda}{12} (g_\sigma \sigma_0)^4 \right] \end{aligned} \quad (\text{C.9})$$

$$\begin{aligned} P &= \frac{1}{3} \langle T_{ii} \rangle = \frac{1}{3} \times 2 \sum_i \int f_{p_i} \frac{p_i^2}{(p_i^2 + M^{*2})^{1/2}} \frac{d^3 p_i}{(2\pi\hbar)^3} + \frac{g_\omega^2}{2m_\omega^2} n^2 \\ &+ \frac{g_\rho^2}{8m_\rho^2} (n_p - n_n)^2 - \frac{1}{2} \left[ m_\sigma^2 \sigma_0^2 + \frac{\kappa}{3} (g_\sigma \sigma_0)^3 + \frac{\lambda}{12} (g_\sigma \sigma_0)^4 \right]. \end{aligned} \quad (\text{C.10})$$

440 The minimization of the grand potential  $\Omega = -PV$  with respect to  $\sigma_0$  (equivalent to  $\partial\epsilon/\partial\sigma_0 = 0$  at  $T = 0$  and to  $\partial P/\partial\sigma_0 = 0$  at finite temperature) leads to

a self-consistent equation for the Dirac effective mass

$$M^* = M - \frac{g_\sigma^2}{m_\sigma^2} \left[ n_s - \frac{\kappa}{2}(M - M^*)^2 - \frac{\lambda}{6}(M - M^*)^3 \right]. \quad (\text{C.11})$$

In the present work we use the masses  $M = 939.0$  MeV,  $m_\sigma = 511.2$  MeV,  $m_\omega = 783.0$  MeV,  $m_\rho = 770.0$  MeV and the couplings  $g_\sigma = 9.061$ ,  $g_\omega = 10.55$ ,  $g_\rho = 7.475$ ,  $\kappa = 9.194$  MeV,  $\lambda = -3.280 \times 10^{-2}$ . These correspond to a cold symmetric nuclear matter equilibrium density  $n_0 = 0.155 \text{ fm}^{-3}$  at which the energy per particle  $E/A = -16$  MeV, the compression modulus  $K_0 = 225$  MeV, and the symmetry energy  $S_v = 30$  MeV.

## References

- [1] G. Baym, C. Pethick, Landau Fermi-Liquid Theory, Wiley Interscience, New York, 1991.
- [2] A. Burrows, J. M. Lattimer, The birth of neutron stars, *Astrophys. J.* 307 (1986) 178–196. doi:10.1086/164405.
- [3] A. Burrows, Supernova neutrinos, *Astrophys. J.* 334 (1988) 891–908. doi:10.1086/166885.
- [4] Y. Sekiguchi, K. Kiuchi, K. Kyutoku, M. Shibata, Gravitational waves and neutrino emission from the merger of binary neutron stars, *Phys. Rev. Lett.* 107 (2011) 051102. doi:10.1103/PhysRevLett.107.051102. URL <http://link.aps.org/doi/10.1103/PhysRevLett.107.051102>
- [5] L. Landau, E. M. Lifshitz, Statistical Physics, Volume 5, Part 1, 3rd Edition, Pergamon, New York, 1980.
- [6] E. M. Lifshitz, L. P. Pitaevskii, Statistical Physics Part 2, Butterworth Heinemann, Oxford, 1980.
- [7] G. Baym, S. A. Chin, Landau theory of relativistic fermi liquids, *Nuclear Physics A* 262 (3) (1976) 527 – 538. doi:http://dx.doi.org/10.1016/0375-9474(76)90513-3. URL <http://www.sciencedirect.com/science/article/pii/0375947476905133>
- [8] J. Blaizot, B. Friman, On the nucleon effective mass in nuclear matter, *Nuclear Physics A* 372 (12) (1981) 69 – 89. doi:http://dx.doi.org/10.1016/0375-9474(81)90087-7. URL <http://www.sciencedirect.com/science/article/pii/0375947481900877>
- [9] D. Coffey, K. S. Bedell, Nonanalytic contributions to the self-energy and the thermodynamics of two-dimensional fermi liquids, *Phys. Rev. Lett.* 71 (1993) 1043–1046. doi:10.1103/PhysRevLett.71.1043. URL <http://link.aps.org/doi/10.1103/PhysRevLett.71.1043>

- [10] C. Constantinou, B. Muccioli, M. Prakash, J. M. Lattimer, Phys. Rev. C, in press; arXiv:1504.03982v1.
- 480 [11] S. Hama, B. C. Clark, E. D. Cooper, H. S. Sherif, R. L. Mercer, Global dirac optical potentials for elastic proton scattering from heavy nuclei, Phys. Rev. C 41 (1990) 2737–2755. doi:10.1103/PhysRevC.41.2737. URL <http://link.aps.org/doi/10.1103/PhysRevC.41.2737>
- [12] P. Danielewicz, R. Lacey, W. G. Lynch, Determination of the equation of state of dense matter, Science 298 (5598) (2002) 1592–1596. arXiv: <http://www.sciencemag.org/content/298/5598/1592.full.pdf>, doi: 10.1126/science.1078070. URL <http://www.sciencemag.org/content/298/5598/1592.abstract>
- 490 [13] P. Demorest, T. Pennucci, S. Ransom, M. Roberts, J. Hessels, A two-solar-mass neutron star measured using shapiro delay, Nature 467 (7319) (2010) 1081–1083. doi:10.1038/nature09466.
- [14] J. Antoniadis, P. C. C. Freire, N. Wex, T. M. Tauris, R. S. Lynch, M. H. van Kerkwijk, M. Kramer, C. Bassa, V. S. Dhillon, T. Driebe, J. W. T. Hessels, V. M. Kaspi, V. I. Kondratiev, N. Langer, T. R. Marsh, M. A. McLaughlin, T. T. Pennucci, S. M. Ransom, I. H. Stairs, J. van Leeuwen, 495 J. P. W. Verbiest, D. G. Whelan, A massive pulsar in a compact relativistic binary, Science 340 (6131). doi:10.1126/science.1233232. URL <http://www.sciencemag.org/content/340/6131/1233232.abstract>
- 500 [15] G. M. Welke, M. Prakash, T. T. S. Kuo, S. Das Gupta, C. Gale, Azimuthal distributions in heavy ion collisions and the nuclear equation of state, Phys. Rev. C 38 (1988) 2101–2107. doi:10.1103/PhysRevC.38.2101. URL <http://link.aps.org/doi/10.1103/PhysRevC.38.2101>
- [16] C. B. Das, S. Das Gupta, C. Gale, B.-A. Li, Momentum dependence of symmetry potential in asymmetric nuclear matter for transport model calculations, Phys. Rev. C 67 (2003) 034611. doi:10.1103/PhysRevC.67.034611. URL <http://link.aps.org/doi/10.1103/PhysRevC.67.034611>
- 505 [17] P.-G. Reinhard, D. J. Dean, W. Nazarewicz, J. Dobaczewski, J. A. Maruhn, M. R. Strayer, Shape coexistence and the effective nucleon-nucleon interaction, Phys. Rev. C 60 (1999) 014316. doi:10.1103/PhysRevC.60.014316. URL <http://link.aps.org/doi/10.1103/PhysRevC.60.014316>
- [18] M. Prakash, T. T. S. Kuo, S. Das Gupta, Momentum dependence, boltzmann-uehling-uhlenbeck calculations, and transverse momenta, Phys. Rev. C 37 (1988) 2253–2256. doi:10.1103/PhysRevC.37.2253. URL <http://link.aps.org/doi/10.1103/PhysRevC.37.2253>
- 515 [19] H. Müller, B. D. Serot, Relativistic mean-field theory and the high-density nuclear equation of state, Nuclear Physics A 606 (1996) 508–537. arXiv: nucl-th/9603037, doi:10.1016/0375-9474(96)00187-X.

- [20] S. Johns, P. J. Ellis, J. Lattimer, Numerical approximation to the thermodynamic integrals, *The Astrophysical Journal* 473 (2) (1996) 1020. doi:10.1086/178212.
- [21] C. Constantinou, B. Muccioli, M. Prakash, J. M. Lattimer, Thermal properties of supernova matter: The bulk homogeneous phase, *Phys. Rev. C* 89 (2014) 065802. doi:10.1103/PhysRevC.89.065802.  
URL <http://link.aps.org/doi/10.1103/PhysRevC.89.065802>